

Effect of uniaxial stress on the electronic state of a platinum-dihydrogen complex in silicon and charge-state-dependent motion of hydrogen during stress-induced reorientation

Y. Kamiura,* K. Sato, Y. Iwagami, Y. Yamashita, and T. Ishiyama

Faculty of Engineering, Okayama University, Tsushima-naka 3-1-1, Okayama 700-8530, Japan

Y. Tokuda

Department of Electronics, Aichi Institute of Technology, Yakusa, Toyota 470-0392, Japan

(Received 10 July 2003; revised manuscript received 11 September 2003; published 28 January 2004)

We have combined isothermal deep-level transient spectroscopy (IT-DLTS) technique with the application of uniaxial compressive stress along $\langle 111 \rangle$ direction to study the effect of stress on the electronic state of a platinum-dihydrogen complex in Si and the kinetics of charge-state-dependent motion of hydrogen around the Pt atom during stress-induced reorientation. We have found that the application of stress splits the IT-DLTS peak into two components and the electronic energy of the short-time component increases linearly with $\langle 111 \rangle$ compressive stress as 35 ± 4 meV/GPa, indicating antibonding character. We have also studied the reorientation kinetics of the complex under the applied stress, and have found that the defect aligned at 78–88 K in the configuration with the smallest activation energy of the level only when the level was not occupied by an electron. This indicates a clear charge-state effect on the local motion of hydrogen around the Pt atom, that is, hydrogen is mobile only in the singly negative charge state of the complex. We have estimated an activation energy 0.27 eV for the hydrogen motion around the Pt atom under a stress of 0.6 GPa. We have examined three structural models, among which a model where the two hydrogen atoms are directly bonded to the platinum atom may be the most plausible candidate. In this structure, defect reorientation needs no bond switching but only the rotation of the whole Pt-H₂ entity. A possible mechanism of the charge-state-dependent reorientation observed may be that if the electronic state with antibonding character is occupied by an electron, the two hydrogen atoms may be displaced outward, probably retarding their motion for the reorientation.

DOI: 10.1103/PhysRevB.69.045206

PACS number(s): 71.55.Cn, 71.70.Fk, 66.30.Jt, 61.72.Yx

I. INTRODUCTION

Platinum is one of the transition-metal impurities that have been known to interact with hydrogen and form various defect complexes in Si. In most cases, such complexes have been detected by deep-level transient spectroscopy (DLTS) since their formation often resulted in the appearance of new electronic levels and/or the disappearance of deep levels associated with transition-metal impurities.^{1–3} However, direct evidence to connect such newly appearing levels to specific defect structures is still lacking, because DLTS provides no structural information. A recent DLTS study combined with depth-profiling technique has proposed that a platinum- and hydrogen-related defect with a deep level at 0.16 eV below the conduction band involves two hydrogen atoms,⁴ but has given no information about the structure of the defect. On the other hand, electron paramagnetic resonance (EPR) is a powerful technique to study the defect structure. Among various Pt- and H-related complexes, a complex named Pt-H₂ was identified to involve two hydrogen atoms and have C_{2v} symmetry by EPR combined with infrared-absorption spectroscopy under uniaxial stress.⁵ In spite of this advantage, EPR could not make the exact determination of energy level of the Pt-H₂ complex, but only gave a rough estimate that the level was located between 0.045 and 0.1 eV below the conduction band.

To obtain the structural information directly connected to the electronic level, we have tried to combine DLTS with the application of uniaxial stress.⁶ The principle is as follows. If a defect has lower symmetry than that of the host lattice and

its deep level is not orbitally degenerate, uniaxial stress lifts the orientational degeneracy of the defect, resulting in the splitting of a DLTS peak. Under the uniform distribution of defects with all the possible orientations in the lattice, the split components of the peak correspond to differently oriented defects with different electronic levels with respect to the applied stress, and the relative peak intensity reflects the ratio of numbers of equivalent orientations. Thus, the stress-induced splitting of a DLTS peak determines the symmetry of the defect.

Our previous experiments showed that $\langle 111 \rangle$ and $\langle 100 \rangle$ stresses split the DLTS peak of the Pt-H₂ complex into two components, and a $\langle 110 \rangle$ stress splits it into three components.⁶ Such a splitting pattern uniquely determined that the complex had orthorhombic symmetry with the C_{2v} point group, from the comparison with the piezospectroscopic theory of Kaplyanskii.⁷ However, the intensity ratios of low- to high-temperature split components were 1.4:1 for $\langle 111 \rangle$ stress, 2.7:1 for $\langle 100 \rangle$ stress, and 1.4:5:1 for $\langle 110 \rangle$ stress, and were not in complete agreement with the theoretical numbers of orientational degeneracy remaining under uniaxial stress for the orthorhombic symmetry, which leads to intensity ratios of 1:1, 2:1, and 1:4:1, respectively. We found that the above discrepancy mainly arose from the stress-induced alignment occurring during the DLTS temperature scan, because we observed that repeated DLTS scans under stress from 65 to 100 K reduced the intensities of high-temperature split components with increasing intensities of low-temperature split components.⁶ Accordingly, we applied isothermal DLTS (IT-DLTS) technique with no tem-

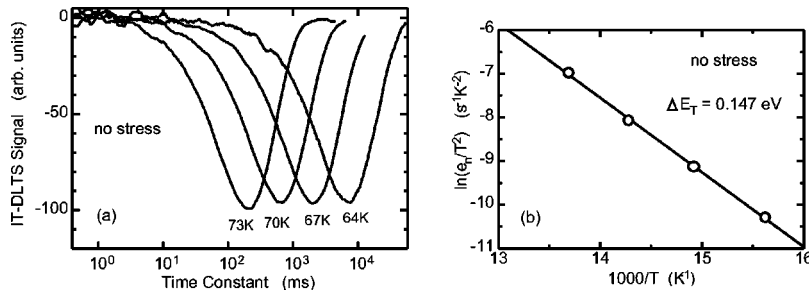


FIG. 1. (a) IT-DLTS spectra taken with no stress at temperatures of 64–73 K. (b) An activation energy ΔE_T for the electron emission from the defect level, determined to be 0.147 eV from Arrhenius plots.

perature scan,⁸ instead of conventional DLTS, at low temperatures of 70 K and below, where hydrogen could not move. IT-DLTS was also combined with the application of uniaxial stress to determine more exact intensity ratios of split components under the condition that hydrogen is immobile.⁹ We have obtained the intensity ratios of short- to long-time split components as 1.1:1 for $\langle 111 \rangle$ stress, 2.3:1 for $\langle 100 \rangle$ stress, and 0.8:3.7:1 for $\langle 110 \rangle$ stress, which are more consistent with the theoretical intensity ratios. We also observed that the Pt-H₂ complex was reoriented above 80 K under uniaxial stress. Such reorientation only occurred when the defect level was not occupied by an electron.⁹ Our observation strongly suggests that the local motion of hydrogen around the Pt atom is remarkably affected by the charge state of the defect, similarly to the hydrogen-carbon (H-C) complex in Si.¹⁰ However, site changes of hydrogen atoms are expected to be much faster in the Pt-H₂ complex than in the H-C complex.

Uftring *et al.* observed a clear effect of the Fermi level on vibrational frequencies of H-stretching modes of the Pt-H₂ complex.⁵ Recently, Weinstein *et al.*¹¹ have indicated from complementary studies by IR absorption and capacitance spectroscopies that several H-stretching lines of the Pt-H₂ complex can be associated with the specific charge states and electronic levels of this defect that was studied by DLTS.^{2–4} All of these studies have strongly suggested an interesting feature of hydrogen dynamics or charge-state-dependent motion of hydrogen in Si.

This paper describes the results of a more extended study of the Pt-H₂ complex in Si by applying IT-DLTS technique combined with the application of uniaxial stress to study the effect of uniaxial stress on the electronic state of the complex and the kinetics of charge-state-dependent motion of hydrogen around the Pt atom during stress-induced reorientation. We have found that the electronic energy of the level varies linearly with $\langle 111 \rangle$ stress and the magnitude of stress dependency depends on the defect orientation with respect to the stress direction. We have also studied the reorientation kinetics of the defect under the applied stress, and have obtained an activation energy 0.27 eV for the hydrogen motion around the Pt atom. We discuss possible structural models and mechanisms of the charge-state-dependent motion of hydrogen observed in the present defect system.

II. EXPERIMENTAL DETAILS

Samples were prepared from a floating-zone silicon crystal, which had a phosphorus density of $6 \times 10^{14} \text{ cm}^{-3}$. For

stress experiments, samples were cut from the crystal into square pillars with dimensions of $1 \times 1 \times 6 \text{ mm}^3$, the longest of which was parallel to the $\langle 111 \rangle$ direction. Platinum was evaporated on one side of samples, which were subsequently annealed at 850 °C for 2 h in an argon ambience for the indiffusion of platinum. Hydrogenation of the platinum-diffused samples was performed by chemical etching (HF:HNO₃:CH₃COOH=1:2:1 or HF:HNO₃=1:10) before the fabrication of Schottky contacts, which were formed by vacuum evaporation of gold on the platinum-diffused side of the samples. A deuterated chemical etchant (HF:DNO₃=1:10) was used to study the isotope effect on hydrogen motion. IT-DLTS measurements were performed at 73 K and below under uniaxial compressive stress of 0.4–0.7 GPa applied to the samples along the $\langle 111 \rangle$ direction. The temperature where capacitance transients were measured was controlled within 0.1 K. The IT-DLTS spectrum was constructed by means of the rate scan method with a bipolar rectangular weighting function.¹² To study the stress-induced defect reorientation, we applied uniaxial stress of 0.6 GPa along the $\langle 111 \rangle$ direction at temperatures of 78–88 K. We also applied reverse bias voltage of 3 V to the Schottky junction during the annealing for stress-induced reorientation to make the defect level unoccupied by an electron, so that the charge state of the Pt-H₂ complex was controlled to the singly negative charge state. Since hydrogen was mobile only in this charge state at 78–88 K,⁹ we applied reverse bias to the sample after taking enough time to stabilize the sample temperature. This enabled us to do short annealing for the defect reorientation, e.g., for a period as short as 1 min. To measure the degree of stress-induced alignment, we carried out IT-DLTS measurements at 70 K under $\langle 111 \rangle$ compressive stress of 0.6 GPa. Other details were the same as published previously.^{6,8–10,12–16}

III. EXPERIMENTAL RESULTS AND ANALYSES

A. Effect of uniaxial compressive stress on the defect level

Figure 1(a) shows typical IT-DLTS spectra with no stress at temperatures T of 64–73 K. We have determined the time constant at a peak by fitting each spectrum to the theoretical curve.⁸ The fitting was very good. The time constant is equal to reciprocal emission rate e_n of an electron from the defect level. In general, e_n is proportional to $T^2 \exp(-\Delta E_T/kT)$, where k is the Boltzmann constant and ΔE_T is an activation energy for the electron emission and is equivalent to the difference between the energy E_c of the conduction-band minima and the energy E_T of the defect level. We can deter-

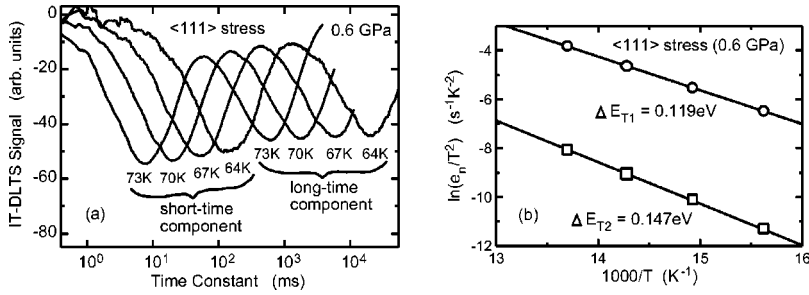


FIG. 2. (a) IT-DLTS spectra taken under a uniaxial stress of 0.6 GPa along the $\langle 111 \rangle$ direction at temperatures of 64–73 K. (b) Activation energies ΔE_{T1} and ΔE_{T2} for electron emission from the defect level, corresponding to short- and long-time components of the split peak, respectively.

mine ΔE_T by constructing so-called Arrhenius plots in Fig. 1(b), where the slope of the line determines ΔE_T to be 0.147 eV, which agrees with that obtained previously by conventional DLTS.⁶ The application of a uniaxial stress of 0.6 GPa along the $\langle 111 \rangle$ direction splits the IT-DLTS peak into two component peaks with almost equal intensities, as shown in Fig. 2(a). The fitting of this spectrum to the theoretical curve was still good.⁹ Activation energies ΔE_{T1} and ΔE_{T2} of short- and long-time components of the split peak, respectively, are determined to be 0.119 eV and 0.147 eV in Fig. 2(b).

We carried out similar IT-DLTS measurements under different magnitudes of $\langle 111 \rangle$ stress, and have obtained stress dependencies of ΔE_{T1} and ΔE_{T2} (Fig. 3). It is seen that ΔE_{T1} linearly decreases with increasing compressive stress P while ΔE_{T2} shows no stress dependency. The decrease of ΔE_{T1} means that the corresponding defect level approaches the conduction band with compressive stress.

Since changes of ΔE_{T1} and ΔE_{T2} include not only the change of the defect level itself but also that of the conduction-band minima, we will subtract the latter from the former to obtain the net energy change of the level in the following way.¹⁷

Considering only the first-order contribution of applied stress, we can write E_c and E_T as

$$E_c = E_{c0} - \delta E_c P \quad (1)$$

and

$$E_T = E_{T0} - \delta E_T P, \quad (2)$$

where a subscript 0 represents the quantities in the unstressed state, and δE_c , δE_T are energy increments per a unit stress.

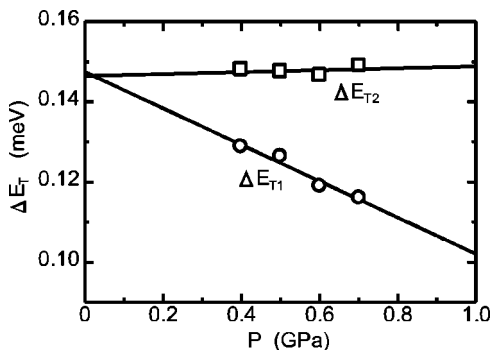


FIG. 3. Dependencies of ΔE_{T1} and ΔE_{T2} on applied compressive stress P .

In Eqs. (1) and (2), the negative sign arises from the compressive nature of P . Using these equations, we can obtain the following equation:

$$\Delta E_{T0} - \Delta E_T = (\delta E_c - \delta E_T) P. \quad (3)$$

Referring to this equation, we have replotted the stress dependencies of Fig. 3 by changing the ordinate to $\Delta E_{T0} - \Delta E_T$ in Fig. 4, where the slopes of lines are written as

$$d(\Delta E_{T0} - \Delta E_T)/dP = -d(\Delta E_T)/dP = \delta E_c - \delta E_T. \quad (4)$$

The values of slopes obtained from Fig. 4 are listed in Table I. To obtain the values of δE_T , we have to subtract $d(\Delta E_{T0} - \Delta E_T)/dP$ from δE_c . On the other hand, stress along the $\langle 111 \rangle$ direction causes no split of the conduction band, and δE_c can be estimated to be 9.6 meV/GPa, based on the deformation-potential analysis.¹⁷ In Table I, the values of δE_T calculated using this value are also shown. In Fig. 4, we also show net shifts $-\delta E_T P$ of the defect level by dashed lines.

B. Stress-induced reorientation of the defect

We have performed a series of isothermal annealing experiments to obtain quantitative results of $\langle 111 \rangle$ -stress-induced reorientation of the Pt-H₂ complex. Figure 5(a) shows IT-DLTS spectra recorded at 70 K under a stress of 0.6 GPa, after successive annealing for the defect reorientation at 85 K with the application of a stress of 0.6 GPa and a reverse bias of 3 V. The figure clearly shows the decrease of the long-time component of the split peak together with the increase of the short-time component, indi-

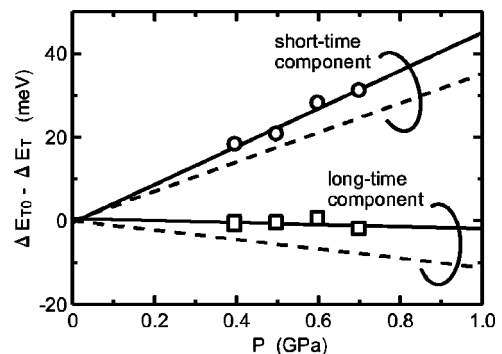


FIG. 4. $\Delta E_{T0} - \Delta E_T$ for short- and long-time components of the split peak, plotted as a function of applied compressive stress P . The stress dependencies of $-\delta E_T P$ calculated using the values of δE_T in Table I are also shown by dashed lines.

TABLE I. Stress-induced shift δE_T of the level of the Pt-H₂ complex. δE_T is calculated by subtracting the slopes of the lines in Fig. 4, $d(\Delta E_{T0} - \Delta E_T)/dP$, from the stress shift δE_c of conduction-band minima. All the above quantities are in meV/GPa.

Split component	Slope	δE_c	δE_T
Short time	45 ± 3	9.6 ± 0.4	-35 ± 4
Long time	-2 ± 2		11 ± 3

cating that defect aligns at 85 K in the configuration under stress with the smallest activation energy. This indicates that the stress-induced increase of gap-state energy of the complex was overcome by the energy gain due to electronic bonding and atomic relaxation, resulting in the decrease of the total energy of the Pt-H₂ complex system. The stress-induced alignment occurred only when the level was not occupied by an electron, which indicates a clear charge-state effect on the local motion of hydrogen around the Pt atom. Under the present bias condition, most of Pt-H₂ complexes were in the singly negative charge state at temperatures of 78–88 K. We observed no changes of IT-DLTS spectra without applying reverse bias, as reported before,⁹ indicating that hydrogen was mobile only in the singly negative charge state of the complex at 78–88 K. Figure 5(b) shows IT-DLTS spectra for the Pt-D₂ complex recorded under the same measurement and annealing conditions as the Pt-H₂ complex. To study the quantitative behavior of stress-induced alignment of defect orientation, we define degree of alignment D as

$$D = (N_1 - N_2) / (N_1 + N_2), \quad (5)$$

where N_1 and N_2 are the densities of Pt-H₂ (Pt-D₂) complexes with configurations corresponding to short- and long-time components of the IT-DLTS peak split under $\langle 111 \rangle$ stress, respectively, and are proportional to the signal intensities of respective components. The signal intensity was determined by fitting each spectrum to the theoretical IT-DLTS curve. If all of the complexes are aligned in the configuration responsible for the short-time component, D is equal to unity, and D reaches zero when the alignment becomes randomized. Figure 5(c) shows annealing-time dependencies of D for both complexes, and clearly indicates the isotope effect on the defect reorientation. This gives strong evidence that hydrogen motion causes the stress-induced reorientation of the Pt-H₂ complex.

We have analyzed the data on the annealing-time dependencies of D using the following reaction scheme,



where k_1 is the rate constant for the reaction of transition from the configuration corresponding to the short-time component of the split peak to that corresponding to the long-time component and k_2 is the rate constant for the reverse reaction. These reactions are controlled by the hydrogen jump between both the configurations, and therefore the rate

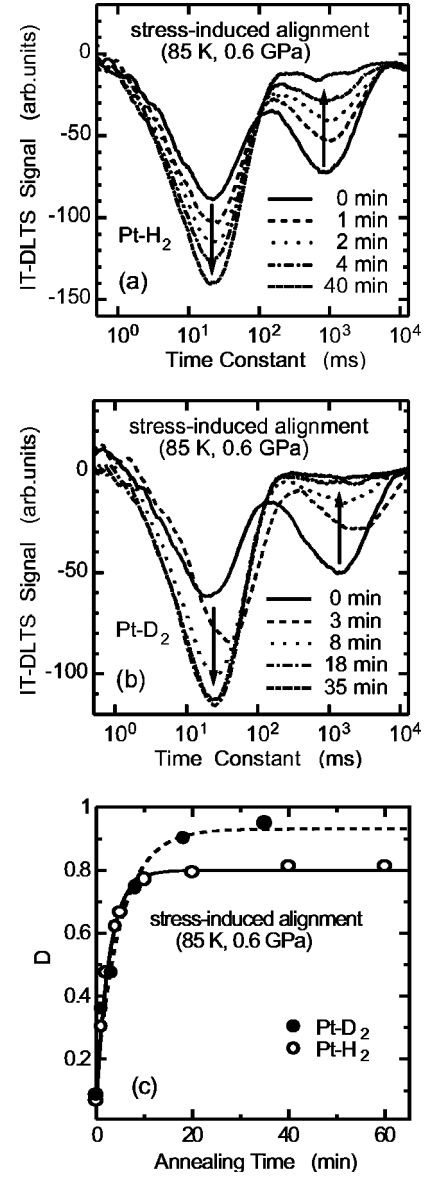


FIG. 5. (a) IT-DLTS spectra recorded at 70 K under a stress of 0.6 GPa, after successive annealing for the defect reorientation of the Pt-H₂ complex at 85 K with the application of a stress of 0.6 GPa and a reverse bias of 3 V. (b) IT-DLTS spectra for the Pt-D₂ complex recorded under the same measurement and annealing conditions as the Pt-H₂ complex. (c) Annealing-time dependencies of degree of alignment D defined by Eq. (5) for both complexes.

constants are equivalent to jump rates of hydrogen (or deuterium). The above scheme leads to the following rate equation:

$$dN_1/dt = -k_1 N_1 + k_2 N_2 = -(k_2 + k_1) N_1 + k_2 N_0, \quad (7)$$

where t is annealing time, and N_0 is the total density $N_1 + N_2$ of split components and remained almost constant with only a few percent of variation during the annealing. This means that hydrogen (or deuterium) jumped from one site to another without little dissociation of the complex. Integration of Eq. (7) gives the solution,

$$N_1 = \frac{k_2}{k_2 + k_1} N_0 + C \exp[-(k_2 + k_1)t], \quad (8)$$

where C is an arbitrary constant. Substituting Eq. (8) into Eq. (5), we obtain

$$D = \frac{2C}{N_0} \exp\left(-\frac{t}{\tau}\right) + D_\infty, \quad (9)$$

where

$$\tau = \frac{1}{k_2 + k_1}, \quad (10)$$

and D_∞ is defined as D at long time enough to achieve the equilibrium in the reaction expressed by Eq. (6). At such long time, $dN_1/dt = 0$ and $k_1 N_1 = k_2 N_2$, and therefore D_∞ is given by

$$D_\infty = \frac{k_2 - k_1}{k_2 + k_1}. \quad (11)$$

We obtained 0.8–0.95 as values of D_∞ in the experiments, indicating that k_1/k_2 is about 0.1 and less. Accordingly, we can ignore k_1 with respect to k_2 to obtain an approximate expression of τ as

$$\tau = \frac{1}{k_2}. \quad (12)$$

For thermally activated motion of hydrogen, k_2 can be written as

$$k_2 = k_{20} \exp\left(-\frac{E_2}{kT_A}\right), \quad (13)$$

where E_2 is an activation energy, k_{20} is a frequency factor, and T_A is annealing temperature. Based on Eqs. (9) and (12), we can determine k_2 for Pt-H₂ and Pt-D₂ complexes from the slopes of plotting $\ln(D_\infty - D)$ vs t [Figs. 6(a) and 6(b), respectively]. Subsequently, we have determined E_2 and k_{20} for the Pt-H₂ complex from Arrhenius plots of k_2 to be 0.27 eV and $6 \times 10^{13} \text{ s}^{-1}$, respectively [Fig. 6(c)]. Although we could not precisely determine E_2 for the Pt-D₂ complex in Fig. 6(c), we have obtained $3 \times 10^{13} \text{ s}^{-1}$ for k_{20} if we use the same value (0.27 eV) of E_2 as that for the Pt-H₂ complex. The values of k_{20} obtained here are consistent with the atomic motion of hydrogen and deuterium.

IV. DISCUSSION

A. Mechanism of charge-state-dependent motion of hydrogen

Our previous results of defect symmetry of the Pt-H₂ complex⁹ are quite consistent with the structural models proposed by Ufring *et al.*,⁵ as shown in Fig. 7. In these models, the substitutional platinum atom is located off-center toward two of its Si neighbors, and two hydrogen atoms terminate the remaining Si bonds, pointing toward the Pt atom (a) or pointing away from it (b). The latter is favored by the authors from their estimate of the Pt-H distance, 0.42 nm, determined from the anisotropy of the hydrogen hyperfine inter-

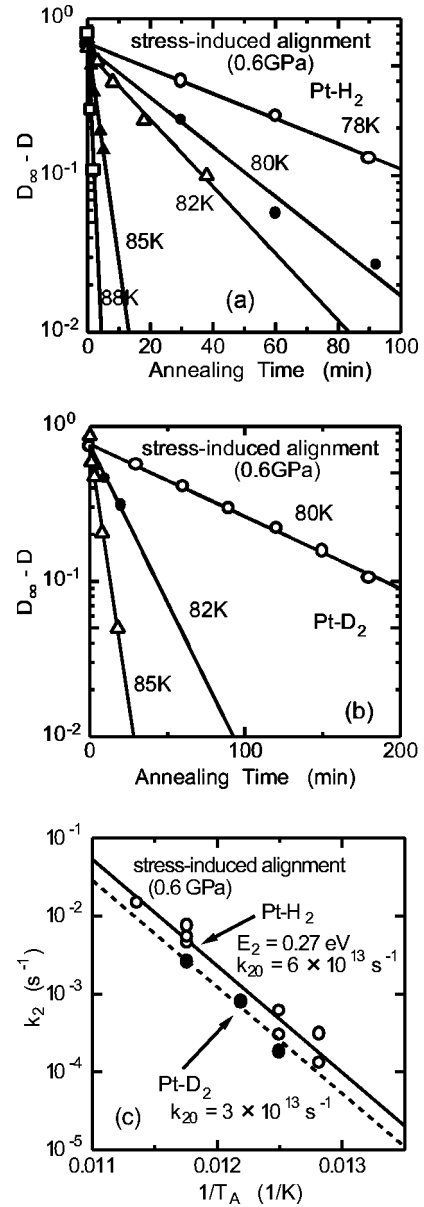


FIG. 6. Plots of $\ln(D_\infty - D)$ vs t for the Pt-H₂ complex (a) and the Pt-D₂ complex (b) at annealing temperatures of 78–88 K to determine k_2 . (c) Arrhenius plots of k_2 . E_2 and k_{20} are determined for the Pt-H₂ complex to be 0.27 eV and $6 \times 10^{13} \text{ s}^{-1}$, respectively. For the Pt-D₂ complex, E_2 is fixed to be 0.27 eV and k_{20} is determined to be $3 \times 10^{13} \text{ s}^{-1}$.

action. Both structures of the complex have a symmetrical axis along the $\langle 100 \rangle$ direction with C_{2v} symmetry.

If the electronic level at $E_c - 0.15 \text{ eV}$ arises from the electronic state whose wave function exists among the Pt atom and two Si neighbors, analogously to the electronic state of isolated substitutional platinum,¹⁸ then the wave function may mainly be distributed along the $\langle 110 \rangle$ axis. Our previous result indicated that the intensity ratio of short- to long-time split components of the IT-DLTS peak was $\approx 2:1$ for $\langle 100 \rangle$ stress.⁹ These short- and long-time components arise from levels with high and low electronic energies, respectively, with respect to the applied stress. Since a particular $\langle 100 \rangle$

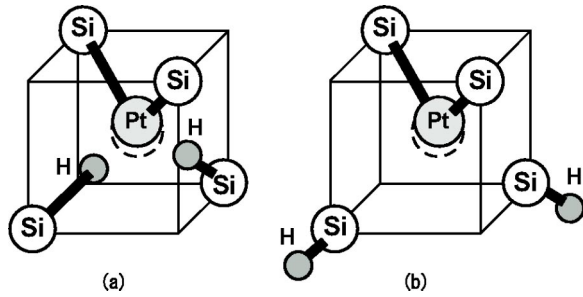


FIG. 7. The structural models proposed by Uftring *et al.* (Ref. 5). In these models, the substitutional platinum atom is located off-center toward two of its Si neighbors, and two hydrogen atoms terminate the remaining Si bonds, pointing toward the Pt atom (a) or pointing away from it (b). Both structures of the complex have a symmetrical axis along the $\langle 100 \rangle$ direction with C_{2v} symmetry.

stress direction has two $\langle 110 \rangle$ axes perpendicular to it and four $\langle 110 \rangle$ axes with an angle of 45° to it, this result strongly suggests that compressive stress to the wave function raises its energy, indicating its antibonding character. This is supported by the stress dependencies of $\Delta E_{T0} - \Delta E_T$ for short- and long-time components shown in Fig. 4, where the energy of the former component increases with increasing stress.

We also found that the stress-induced reorientation of the Pt-H₂ complex only occurred when the level was not occupied by an electron.⁹ This observation strongly suggests that the local motion of hydrogen around the Pt atom is remarkably affected by the charge state of the defect and hydrogen moves preferentially in the singly negative charge state of the complex. The charge state of the complex is controlled by the occupation of an electron at the gap state whose wave function may be distributed among the Pt atom and two Si neighbors, where however hydrogen atoms do not exist. It has been known that the reorientation of isolated substitutional platinum occurs at very low temperatures.¹⁸ The experimentally observed charge-state-dependent motion of hydrogen suggests that such Pt motion should affect hydrogen motion. Therefore, our results favor the structural model of Fig. 7(a), where two hydrogen atoms exist nearer to the Pt atom. In this case, a possible mechanism of electronically induced motion of hydrogen may be as follows. The off-centered Pt atom is first displaced in the electron-empty gap state of the Pt-H₂ complex, probably moving apart from the two Si neighbors bonding to Pt and nearer to the hydrogen atoms. In this atomic configuration, the bond switching of the Pt atom from one of the Si neighbors bonding to Pt to another not bonding to it occurs more easily to induce hydrogen motion for defect reorientation. In the electron-occupied gap state with antibonding character, the Pt atom may be relaxed toward the two Si neighbors, retarding the bond switching.

Apart from the two models proposed by Uftring *et al.*, we can also consider the third model where the two hydrogen atoms are directly bonded to the platinum atom (Fig. 8). This model has two sets of two silicon atoms that are displaced inward to make a bond. The Pt-H₂ entity is located between the two sets. The model has a symmetrical axis along the $\langle 100 \rangle$ direction with C_{2v} symmetry. Defect reorientation

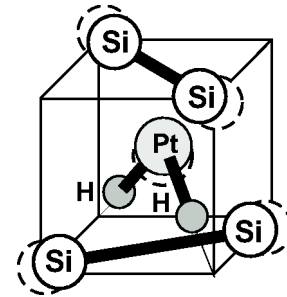


FIG. 8. The third structural model to be considered here. The two hydrogen atoms are directly bonded to the platinum atom. There are two sets of two silicon atoms that are displaced inward to make a bond. The Pt-H₂ entity is located between the two sets. This model has a symmetrical axis along the $\langle 100 \rangle$ direction with C_{2v} symmetry.

needs no bond switching but only the rotation of the whole Pt-H₂ entity. This may well fit with the present results that the reorientation occurs very easily with a low activation energy. Analogously to the above two models, it is reasonable to assume that the electronic level at $E_c - 0.15$ eV arises from the electronic state whose wave function is distributed among the platinum atom and two hydrogen neighbors along the $\langle 110 \rangle$ axis. This is consistent with the antibonding character of the electronic state and its stress dependencies. If the electronic state with antibonding character is occupied by an electron, the two hydrogen atoms may be displaced outward, probably retarding their motion for the reorientation. From the above discussion, this model may be the most plausible candidate.

B. Energetics of stress-induced reorientation

Figure 9 shows the schematic illustration of energetics of hydrogen motion in the stress-induced reorientation of the Pt-H₂ complex under stress. C_1 and C_2 represent the configurations of the complex corresponding to short- and long-time components of the split IT-DLTS peak under stress,

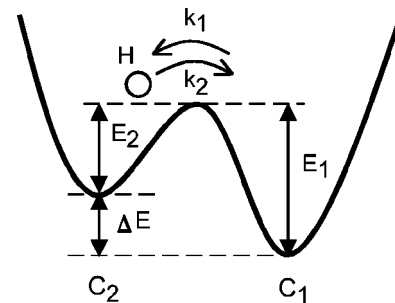


FIG. 9. Schematic illustration of energetics of hydrogen motion in the stress-induced reorientation of the Pt-H₂ complex under stress. C_1 and C_2 represent the configurations of the complex corresponding to short- and long-time components of the split IT-DLTS peak under stress, respectively. E_1 and E_2 are energy barriers for hydrogen jumps from configurations C_1 and C_2 , respectively, and ΔE is the energy difference between C_1 and C_2 configurations. E_1 , E_2 , and ΔE are estimated to be 0.29, 0.27, and 0.02 eV, respectively, for a $\langle 111 \rangle$ compressive stress of 0.6 GPa.

respectively. E_1 and E_2 are energy barriers for hydrogen jumps from configurations C_1 and C_2 , respectively, and ΔE is the energy difference between C_1 and C_2 configurations. In the preceding section, E_2 has been determined to be 0.27 eV for a $\langle 111 \rangle$ compressive stress of 0.6 GPa. ΔE can be estimated in the following. At sufficiently long time to achieve the equilibrium in the reaction expressed by Eq. (6), the following equation holds:

$$\frac{N_2}{N_1} = \frac{k_1}{k_2} = \frac{k_{10}}{k_{20}} \exp\left(-\frac{\Delta E}{kT_A}\right), \quad (14)$$

where k_{20} is a frequency factor of k_2 . Here, we rewrite Eq. (11) as

$$\frac{k_1}{k_2} = \frac{1 - D_\infty}{1 + D_\infty}. \quad (15)$$

We can therefore estimate ΔE by plotting logarithm of $(1 - D_\infty)/(1 + D_\infty)$ against reciprocal annealing temperature. However, we have not been able to obtain any meaningful results because of scatter of data points. Accordingly, we have estimated it directly using Eqs. (14) and (15), assuming that k_{10} and k_{20} have the same magnitude. An estimated value is 16 ± 3 meV for the experimentally obtained value of D_∞ , 0.82 ± 0.05 . This value (27 meV/GPa) can be compared with that (23 meV/GPa) reported for the boron-hydrogen complex in Si.¹⁹ In summary, we have estimated E_1 , E_2 , and ΔE to be 0.29, 0.27, and 0.02 eV, respectively, for a $\langle 111 \rangle$ compressive stress of 0.6 GPa.

V. SUMMARY

We have combined IT-DLTS technique with the application of uniaxial compressive stress along $\langle 111 \rangle$ direction to study the effect of stress on the electronic state of a platinum-dihydrogen complex in Si and the kinetics of charge-state-dependent motion of hydrogen around the Pt atom during stress-induced reorientation. We have found that the electronic energy of the level varies linearly with $\langle 111 \rangle$ stress and the magnitude of stress dependency depends on the defect orientation with respect to the stress direction.

Subtracting the stress shift of the conduction-band minima from that of the activation energy for electron emission from the defect level, we have obtained 35 ± 4 meV/GPa as a net increase in electronic energy for the defect orientation with the smallest activation energy. This result strongly suggests that compressive stress raises the energy of the electronic state of the Pt-H₂ complex, indicating its antibonding character.

We have also studied the reorientation kinetics of the complex under the applied stress, and have found that the defect aligned at 78–88 K in the configuration with the smallest activation energy of the level. This indicates that the stress-induced increase of gap-state energy of the complex was overcome by the energy gain due to electronic bonding and atomic relaxation, resulting in the decrease of the total energy of the Pt-H₂ complex system. The stress-induced alignment occurred only when the level was not occupied by an electron, indicating a clear charge-state effect on the local motion of hydrogen around the Pt atom, that is, hydrogen was mobile only in the singly negative charge state of the complex. We have estimated an activation energy 0.27 eV for the hydrogen motion around the Pt atom under a stress of 0.6 GPa.

We have discussed a possible mechanism of the charge-state-dependent motion of hydrogen observed in the present defect system. We have examined three structural models, among which a model where the two hydrogen atoms are directly bonded to the platinum atom may be the most plausible candidate, because defect reorientation needs no bond switching but only the rotation of the whole Pt-H₂ entity. This may well fit with the present results that the reorientation occurs very easily with a low activation energy. If the electronic state with antibonding character is occupied by an electron, the two hydrogen atoms may be displaced outward, probably retarding their motion for the reorientation.

ACKNOWLEDGMENT

This work was supported in part by a Grant-in-Aid for Scientific Research (Grant No. 15340099) from the Ministry of Education, Culture, Sports, Science and Technology.

*Electronic address: kamiura@ms.elec.okayama-u.ac.jp

¹T. Sadoh, K. Tsukamoto, A. Baba, D. Bai, A. Kenjo, and T. Tsurushima, *J. Appl. Phys.* **82**, 3828 (1997).

²J.-U. Sachse, E.O. Sveinbjornsson, W. Jost, J. Weber, and H. Lemke, *Phys. Rev. B* **55**, 16 176 (1997).

³N. Yarykin, J.U. Sachse, H. Lemke, and J. Weber, *Phys. Rev. B* **59**, 5551 (1999).

⁴J.-U. Sachse, J. Weber, and E.O. Sveinbjornsson, *Phys. Rev. B* **60**, 1474 (1999).

⁵S.J. Uftring, M. Stavola, P.M. Williams, and G.D. Watkins, *Phys. Rev. B* **51**, 9612 (1995).

⁶K. Fukuda, Y. Iwagami, Y. Kamiura, Y. Yamashita, and T. Ishiyama, *Physica B* **308-310**, 240 (2001).

⁷A.A. Kaplyanski, *Opt. Spectrosc.* **16**, 329 (1964).

⁸Y. Tokuda, K. Kamiya, and T. Okumura, *J. Appl. Phys.* **88**, 1943 (2000).

⁹Y. Kamiura, Y. Iwagami, K. Fukuda, Y. Yamashita, T. Ishiyama, and Y. Tokuda, *Microelectron. Eng.* **66**, 352 (2003).

¹⁰Y. Kamiura, K. Fukuda, Y. Yamashita, and T. Ishiyama, *Phys. Rev. B* **65**, 113205 (2002).

¹¹M.G. Weinstein, M. Stavola, K.L. Stavola, S.J. Uftring, J. Weber, J.-U. Sachse, and H. Lemke, *Phys. Rev. B* **65**, 035206 (2001).

¹²Y. Tokuda, N. Shimizu, and A. Usami, *Jpn. J. Appl. Phys., Part 1* **18**, 309 (1979).

¹³M. Yoneta, Y. Kamiura, and F. Hashimoto, *J. Appl. Phys.* **70**, 1295 (1991).

¹⁴Y. Kamiura, M. Hayashi, Y. Nishiyama, S. Ohyama, and Y. Yamashita, *Jpn. J. Appl. Phys., Part 1* **36**, 6579 (1997).

- ¹⁵Y. Kamiura, N. Ishiga, and Y. Yamashita, *Jpn. J. Appl. Phys., Part 2* **36**, L1419 (1997).
- ¹⁶K. Fukuda, Y. Kamiura, and Y. Yamashita, *Physica B* **273-274**, 184 (1999).
- ¹⁷K. Fukuda, Y. Kamiura, Y. Yamashita, and T. Ishiyama, *Jpn. J. Appl. Phys., Part 1* **40**, 6700 (2001).
- ¹⁸F.G. Anderson, R.F. Milligan, and G.D. Watkins, *Phys. Rev. B* **45**, 3279 (1992).
- ¹⁹I.A. Veloarisoa, M. Stavola, Y.M. Cheng, S.J. Uffring, and G.D. Watkins, *Phys. Rev. B* **47**, 16 237 (1993).